

THE ROLE OF NIOBIUM IN AUSTENITIC AND DUPLEX STAINLESS STEELS

David Dulieu

Consultant,
20 Topside, Grenoside
Sheffield, S35 8RD, United Kingdom

Abstract

The two principal roles of niobium in cast and wrought austenitic stainless steels are as a stabilising agent to reduce the risk of intergranular corrosion and as a strengthening agent. To date there appears to be no parallel roles in the duplex, austenitic-ferritic stainless steels. The principles for designing an austenitic steel composition are outlined and the effects of niobium as an alloying element summarised. The characteristics of the principal precipitate phases and their occurrence are reviewed in the context of service requirements, to illustrate how compositions have evolved. Metallurgical developments covered include the benefits derived from a balanced reduction in the levels of niobium and carbon in the 347 composition. Application of controlled heat treatments combined with cold working has allowed optimisation of both steam-side oxidation and creep strength for this widely used grade. The combination of low levels of niobium with enhanced nitrogen additions has led to alternative stabilisation mechanisms. Enhanced precipitation strengthening for high temperature applications derives from multiple microalloying additions of, principally, niobium, titanium and vanadium and recognition of the role of the chromium-niobium nitride. Families of high strength creep resisting steels have been developed for both fossil and nuclear power generation applications, based on the synergistic effects of multiple alloying additions of molybdenum, niobium, titanium, nitrogen, copper and tungsten. These steels exploit knowledge of alloy design to combine effective solid solution and precipitation strengthening with optimum grain boundary precipitation.

Introduction

Background and History

The majority of niobium-bearing austenitic steels fall into two major classes: steels with stabilising additions to prevent intergranular corrosion and compositions for elevated temperature service. The latter can be subdivided into those with niobium as the principal addition enhancing creep strength, and more complex alloys using the interactive effects of other additions. Although this review covers primarily wrought alloys, many individual grades are available as castings. The development of the niobium-bearing steels has been linked closely to applications within power generation, chemicals, nuclear and gas turbine technologies. Binder (1) gave a comprehensive review of the field in 1957, a time when adoption of the 347 grade in the superheater and other high temperature areas of steam power plant had focused attention on several issues. These included hot-workability, problems of liquation and stress-relief cracking on welding and cast and product form variability of elevated temperature properties. By the time of the review by Keown and Pickering (2) in 1981, the variability in behaviour of niobium-bearing steels was in large measure understood. The importance of the temperature and compositional dependence of the solubility of Nb(C,N) was established and effects of supersaturation, cold work, and ageing or stabilising heat treatments on secondary precipitation had been related to the behaviour of weld and parent metals.

The present review does not attempt to cover all the more recent compositional variants or applications. The starting-point is to consider the selection of the basic iron-chromium-nickel-(manganese-nitrogen) matrix, within which niobium will play its role. Examples of the various niobium-containing compositions are then introduced. The effects of niobium as an alloying element are summarised and the precipitate phases and precipitation sequences in both wrought and cast alloys outlined in relation to service requirements. Aspects of oxidation and the role of niobium in steels subject to irradiation are then considered. Unless specified, descriptions of steels such as '347' used in this text are generic terms and not specific, standardised grade descriptions; the references cited should be consulted for further details. All compositions are given in weight %.

Metallurgical Developments

Important metallurgical aspects of developments in niobium-bearing steels which are reflected in the work reviewed fall under the following headings :

- The benefits for hot workability, ductility and weldability to be gained from minimising the volume fraction of primary carbide particles.
- The importance of additional carbide-forming elements such as titanium in extending the effectiveness of the niobium-based MC precipitates in high temperature steels.
- Recognition of the significant effects of low levels of niobium additions, especially when present in steels with enhanced nitrogen levels, in relation to strength and intergranular corrosion resistance.
- The exploitation of mixed intragranular precipitate populations for creep strength.
- The stability of Nb(C,N) versus the Z-phase (Cr,Nb) nitride and 'secondary' chromium carbides in relation to strengthening effects in the higher nitrogen steels.
- Control over precipitate distribution and the balance between inter- and intragranular precipitation. This to optimise creep rupture life, in both low and high carbon-niobium alloys across a range of service temperatures.
- Optimisation of the roles of alloying elements in irradiated microstructures.

The Iron-Chromium-Nickel Matrix and the Roles of Alloying Elements Found in Austenitic and Duplex Stainless Steels

Austenitic Steels

The basic physical metallurgy of austenitic stainless steels has been summarised by Harries (3). Stainless steels have chromium as their principal addition. In austenitic stainless steels the effective lower limit is around 13%. The upper limit rarely exceeds 25% and is set by the tendency to form the sigma Fe-Cr intermetallic phase on thermal exposure, or the behaviour of high chromium steels in specific aggressive environments. Silicon and aluminium promote oxidation resistance and are ferrite stabilisers. Rare earth additions may be used to improve oxide stability. For elevated temperature strength additions of nitrogen, molybdenum and tungsten are used, together with elements forming stable intragranular precipitates on a scale inhibiting dislocation movement.

For corrosion resistance at relatively low temperatures, the protective, passive oxide film must not be weakened by localised matrix chromium depletion. A decision will be made, based on fabrication route and service exposure, on the need for a stabilising addition of either titanium or niobium versus use of a low carbon grade. Pitting resistance is enhanced by additions of molybdenum, tungsten and nitrogen.

Having established an oxidation or corrosion-resistant composition, a nickel addition, or less often a combined nickel-manganese-nitrogen addition, can then be chosen to promote the formation of an austenitic structure. Factors determining the level of austenite stabilisers include:

- Hot workability considerations, the need for a controlled solidification path.
- Stability of the structure in respect of transformation during work-hardening and at low temperatures, need to achieve low magnetic permeability.
- The beneficial effects of nickel for reducing carburisation and nitridation rates.
- Susceptibility to sigma phase formation and changes in matrix and grain boundary region compositions arising from precipitation at elevated temperatures.

The matrix compositions of most of the niobium-bearing steels fall in the ranges 15-25%Cr, 9-35%Ni. Nickel and chromium equivalents can be used to predict solidification structures. For example, Kotecki and Siewert (4) summarised weld structure prediction models derived from the original Schaeffler Diagram and gave a factor of 0.7 for the chromium equivalent of niobium. Phase diagrams are supplemented by calculations from thermodynamic data for prediction of equilibrium phase stability.

Of the minor elements in austenitic stainless steels, sulphur may segregate to grain boundaries at high temperatures and is deleterious to pitting corrosion resistance. It is kept to low levels (<0.005%) in most modern production. Phosphorus has a specific role in certain precipitation sequences but is usually kept low in alloys requiring high intergranular corrosion resistance, see for example, Kajimura *et al.* (5).

Duplex Steels

The duplex stainless steels (6) are balanced compositionally to develop equal amounts of austenite and ferrite in the microstructure, while avoiding the formation of intermetallic phases during fabrication. They have the advantages of increased strength over the lower alloy austenitic compositions, of good pitting and stress corrosion cracking resistance and nickel contents lower than in their austenitic equivalents.

The scope for niobium additions to the duplex steels as presently formulated appears to be limited. Corrosion behaviour, in terms of sensitisation effects, is influenced largely by the need to avoid intermetallic phases, rather than chromium carbides. Rossitti and Rollo (7) found that a 0.5% niobium addition to a 26%Cr, 6%Ni, 3%Mo, 3%Cu, 0.2%N duplex steel resulted in a very high ferrite content on solution annealing. However, this ferrite decomposed rapidly to austenite and sigma phase on ageing with a pronounced hardening response. Tacke and Kohler (8) studied experimental duplex stainless steels with 0.2-0.25%N, 0.2% niobium and 0.2% vanadium. They found extensive nitride formation and a significant variation in particle size for the intragranular niobium-bearing (Z-phase) precipitates between the ferrite and austenite. The susceptibility to precipitation of intermetallic phases is considered to limit the application of the conventional duplex steels at elevated temperatures, so there is little incentive to seek to optimise intragranular precipitation within the two phases for creep strength.

Standard and Special-purpose Niobium-bearing Austenitic Stainless Steels

Almost all standards include steels of nominal compositions 18%Cr, 10%Ni and 17%Cr, 11%Ni, 2-3%Mo, with a stabilising niobium addition. These '347' and '316Nb' grades have, typically, a maximum permitted carbon content of 0.08% and a niobium factor of x10 with a maximum niobium content of 1.0-1.2wt%. Table 1 gives examples of variants of these grades, together with examples of Cr-Ni-Mn compositions for internal combustion engine valve (9) and non-magnetic applications. Many other corrosion and heat resisting standard steels have niobium stabilised variants. However, none of the major standards appear to list a niobium-bearing duplex steel.

Examples of other wrought niobium bearing steels for elevated temperature service are given in Table 2. The steels in Table 2 are laid out nominally in chronological order and by chromium content and composition. They illustrate the use of combined strengthening mechanisms, in the approximate sequence from Mo-Nb, Mo-V,Ti,Nb to Mo-Nb,Ti-Cu, Mo-Nb-N and W-Nb-Cu. The nickel and chromium levels indicate the balance sought between oxidation resistance and sigma phase susceptibility.

Table I Examples of standard wrought and cast Nb-bearing austenitic Cr, Ni, Mo stainless steels

Common Designation	Wt% C	Cr	Ni	Mo	N	Nb	Other	Typical Standard Designation
'347'	0.08	17.0-19.0	9.0-12.0			10xC min, to 1.00		EN 10088-1, 1.4550
'347H'	0.04-0.10	17.0-19.0	9.0-13.0			8xC min, To 1.00		ASTM A240, S34709
'347L'	0.03	19.0-21.5	9.00-11.00				Mn, 1.0-2.5	J SUS Y 347L
347LN	0.005-0.020	17.0-20.0	9.0-13.0		0.06 - 0.10	(Nb+Ta)>15xC		ASTM A213M-99a S34751
'16-13Nb'	0.04-0.10	15.0-17.0	12.0-14.0			10xC min, to 1.20	Si, 0.30-0.60	EN 10028-7, prEN 10302, 1.4961
'348'	0.08	17.0-19.0	9.0-13.0			(Nb+Ta)10xC min, to 1.00, Ta <0.1	Co <0.2	ASTM A240 S34800
'316Nb'	0.06		11.0-13.0	2.50-3.00		(Nb+Ta)10xC min, to 1.00, Nb/C <25		F Z6CNDNb 18-12
JS700	0.04	19.0-23.0	24.0-26.0	4.3-5.0		>8C, <0.4		N08700
Auto Valve steel	0.48-0.58	20.0-22.0	3.25-4.5		0.38 - 0.50	(Nb+Ta), 2.0-3.0	Mn, 8.0-10.0 (C+N) 0.9	1.4870
Non-magnetic	0.03	21.0-24.5	15.5-18.0	2.8-3.4	0.3-0.5	0.1-0.3	Mn, 4.5-6.5	1.3974
Castings	0.05-0.15	19.0-21.0	31.0-33.0			0.5-1.5		1.4859
	0.25-0.4	23.0-25.0	23.0-25.0			1.20-1.80	Si, 0.5-2.0	1.4855
Mod.HK 40	<i>0.45</i>	<i>25</i>	<i>20</i>			<i>0.6</i>	<i>Ti, 0.15</i>	Ref.(68)

(In all tables, composition ranges are quoted from the standards or references given. A single figure denotes the maximum level. Figures *in italics* denote 'typical compositions' as quoted in literature references. Unless indicated, most steels have minor element contents below the following levels, Si 1.0, Mn 2.0, P 0.03 and S 0.01.)

Table II Examples of wrought creep resisting Nb-bearing austenitic Cr, Ni, stainless steels

Designation	Wt% C	Cr	Ni	Mo	N	Nb	Ti	Others	B	Ref.
FV 548	0.06-0.09	16.0-17.0	11.0-12.0	1.5	0.015	1.05			0.001-0.003	(3)
E1250	0.06-0.15	14.0-16.0	9.0-11.0	0.8-1.2		0.75-1.25		Mn, 5.5-7.0, V, 0.15-0.4	0.003-0.009	BS3605 :1 215S15
Tempaloy A-1	0.07-0.14	17.5-19.5	9.0-12.0			<0.40 Ti+Nb/2/ 2 (0.6-2.5)	<0.20		0.001-0.004	(29)
ONRL 'HT-UPS' Mod.316	0.08	14-16	16	2.5	<0.02	0.1	0.3	Mn, 2 Cu, 0-2, V, 0.1-0.5, Si, 0.4, P, 0.02- 0.07	0.005-0.007	(30)
17-14CuMo	0.12	16.0	14.0	2.0		0.4	0.3	Cu, 3.0	0.006	(63)
Super 304H	0.07-0.13	17.0-19.0	7.5-10.5		0.05-0.12	0.3-0.6		Cu 2.5-3.5		(65)
Tempaloy AA-1	0.07-0.14	17.5-19.5	9.0-12.0			<0.40	<0.25	Cu 2.50-3.50	<0.005	(29)
Rex 734	0.05	20.6	9.5	2.80	0.38	0.27		Mn, 3.6		(34)
HR3C	0.10	23.0-27.0	17.0-23.0		0.15-0.35	0.20-0.60				(59)
Tempaloy A-3	0.03-0.10	21.00-23.00	14.50-16.50		0.10-0.20	0.5-0.80			<0.005	(29)
20-25-Nb	0.02	19.0-21.0	24.0-26.0			8x(C+N)				(37,38)
NF709	0.04-0.10	19.0-22.0	23.0-27.0	1.0-2.0	0.10-0.20	0.10-0.40	0.02-0.20		0.002-0.008	(62)
HT-UPS mod.800H	0.09	20.4	30.4	2.0	0.028	0.24	0.36	V, 0.53, P, 0.045	0.01	(31)
SAVE25	0.1	23	18.0		0.2	0.45		Cu, 3.0, W, 1.5		(49)

Niobium as an Alloying Element

Solidification and Reheating Considerations

Folkhard (10) quoted the solubility of niobium in the austenite of pure iron as 4.1% at 1300°C. The principal iron-niobium phase is the Laves, Fe₂Nb and the melting points of the eutectics NbC-austenite and Fe₂Nb-delta iron were given as 1315 and 1370°C respectively. Denham and Silcock (11) estimated that, in a 16%Cr, 16%Ni steel, the Laves phase solubility was approximately 2.4% at 1250°C and an addition of 1% silicon reduced this to around 1.6%. Ramanathan *et al.* (12) studied 15%Cr, 15%Ni steels with 0.03% carbon or less and 0.4%Si. After solution treatment at 1200°C, they found only traces of Laves phase in a steel containing 1.88% Nb. Kirman (13) studied 15%Cr 16-59%Ni alloys with 2.5-7% niobium and found that the solubility of the Laves phase increased with nickel content.

Solidification of an austenitic steel may involve the initial formation of ferrite, some of which may be retained in the solid structure on cooling. The solidification routes, described in (14) and by Boothby (15), may be broadly via primary ferrite formation, primary ferrite and austenite formation, or primary austenite formation. Primary ferritic solidification is beneficial for hot ductility in initial processing and for the avoidance of cracking on welding. In (14) solidification data were presented for a Type '316Nb' steel, (0.052%C, 0.54%Nb and 0.010%N with a Cr_{eq}/Ni_{eq} ratio of 1.58). The NbC-austenite eutectic was formed at 1330°C. The carbide formation range was given as extending to the solidus temperature, varying from 1305 to 1275°C over the cooling rate range 0.1-2.0°C/sec. Solid state precipitation of NbC was also noted, nucleating on dendritic ferrite.

Lundin (16) reviewed weldability aspects of the austenitic stainless steels. He proposed using a Cr/Ni equivalent ratio for solidification >1.6 to reduce the risk of base metal HAZ hot cracking and lowering the niobium and carbon levels to reduce eutectic formation. For steels of the 347 type, base metal HAZ liquation cracking could be minimised by adopting the following working relationships:

$$\frac{0.5Nb\%}{(30C\%+50N\%)} < 0.1, \quad Nb\% > 13C\%. \quad (1)$$

Primary niobium carbide present after working and heat treatment will behave as an inclusion phase. Lee *et al.* (17) were able to detect a dependence of the fracture toughness of the SA312-TP347 grade on the presence of coarser NbC particles, as reflected in the carbon, niobium and nitrogen contents. Toughness was measured at 316°C by the J-integral technique on samples of reactor coolant circuit pipework. Although no quantitative particle population data were presented, the toughness was higher in a 0.04%C, 0.45%Nb, 0.06%N, than in a 0.06%C, 0.78%Nb, 0.12%N steel.

Niobium in Solid Solution

Niobium has a relatively high atomic mass number of 93 and atomic radius larger than iron, nickel and chromium. Kato *et al.* (18), reported measured atomic volume size factors for vanadium, titanium, niobium in a 316L matrix of 10, 37 and 62% respectively. Martinez *et al.* (19) determined by X-ray diffraction the effect of additions of niobium up to 1.74% on the stacking-fault energy of a low carbon, low nitrogen 15%Cr, 15%Ni matrix. They found that the SFE fell from 46 to 23mJ/m² for an addition of 1% niobium. This was attributed to the lower electron/atom ratio of the addition, causing an increase in the mean electron vacancy number.

Significant effects on creep strength can be detected from niobium present as a trace impurity at 0.1% and lower levels, as discussed for example by Moorhead and Sikka, cited in Marshall and Farrar (20). The latter showed how these low niobium levels may arise by transfer to weld metal from rutile electrode coatings.

The Principal Precipitating Phases

Niobium is used primarily to lower the solubility of carbon in austenite and to form stable particle dispersions. The principal relevant phases formed in niobium-bearing steels are introduced below and more detailed information is given in the review of precipitation in creep resistant austenitic steels by Sourmail (21).

Niobium Carbides and Nitrides

'MC' or 'MX', $(\text{Nb,Ti,V,Zr,Cr})(\text{C,N})_x$ embraces the range of carbides and carbo-nitrides with a cubic structure, varying in approach to stoichiometry, which have been reported in austenitic steels containing additions of niobium, singly or with titanium, vanadium and zirconium. With niobium only and a relatively high ratio of carbon to nitrogen, the phase formed at high temperatures is basically NbC. Lattice parameter measurements by Deighton (22) indicated that the insoluble carbides present in high purity 20%Cr, 25%Ni,Nb steels with low nitrogen levels were $\text{NbC}_{0.95-0.97}$.

Sundman *et al.* cited in (23) used the Thermo-Calc system to estimate that 20% of the total volume fraction of NbC in a 347 steel, (0.054%C, 0.78%Nb, 0.02%N), was present as primary carbide forming at 1360°C and that carbide formation was substantially complete at 550°C. The prediction indicated that over 50% of the carbide was out of solution at 1200°C and 85% at 1000°C. Källqvist and André (23,24) analysed the MC particles present in this steel. The tube material was solution annealed at 1100°C, water quenched and then aged for times in excess of 45kh at temperatures of 500, 600 and 700°C. The niobium content of the coarser (2.5 μm) particles present was greater than 89%, with 4.5%Fe and 2-2.5%Cr. Källqvist (25) indicated compositions of $\text{Nb}(\text{C}_{0.88}\text{N}_{0.12})_{0.9}$ and $\text{Nb}(\text{C}_{0.68}\text{N}_{0.32})_{0.8}$ for the primary MX and the finer (40nm) particles present after ageing at 700°C. André *et al.* (26) found that in the initial stages of precipitation the 'NbC' is sub-stoichiometric and enriched in chromium. Källqvist and André (24) found that niobium depletion of the matrix was substantially complete after 800h at 700°C. Precipitation was very slow at 500°C, with significant amounts of niobium and carbon left in the matrix after 46,675h. Nb-N clusters or very small precipitates were detected by atom probe field microscopy (APFIM), with the suggestion that these are precursors to NbX precipitation at this temperature.

The effect of the nitrogen to carbon ratio on the composition of MC is illustrated by the report by Diglio *et al.* (27) of the composition $\text{Nb}(\text{C}_{0.45}\text{N}_{0.55})$ for the phase undissolved at 1150°C in a modified 800H (20%Cr-32%Ni) composition with 0.075%C, 1.44%Nb, 0.12%N. Schwind *et al.* (28), found that nitrogen pick-up during creep testing at 800°C for 77,782h resulted in the replacement of carbon by nitrogen in the NbC particles in a 347 steel. Liberation of carbon into the matrix led to formation of M_{23}C_6 carbide.

Alloying additions modify the solubility and stability of 'MX' precipitates. Tohyama and Minami (29) proposed, on the basis of lattice parameter measurements that the MC phase found in the Tempaloy A-1, Nb-Ti steel (Table 2) contained equal amounts of niobium and titanium. $(\text{Nb}_{0.5}\text{Ti}_{0.5})\text{C}$. Maziasz (30) explored MC phase formation in 14%Cr-16%Ni-2.5%Mo 'HT-UPS' alloys. Combined additions of Nb, Ti and V, all soluble in the MC phase were found to confer maximum resistance to MC particle coarsening. Studies on (Mo,V,Ti,Nb)C precipitates in Alloy 800H variants by Swindeman and Maziasz (31) indicated a destabilisation of the MC phase as the matrix chromium level increased from 20 to 25%. Thorvaldsson and Dunlop (32) analysed mixed, (V,Nb) MX precipitates formed in 17%Cr, 12.5%Ni alloys with varying C:N ratios. They detected significant levels of chromium, enhanced by the high levels of nitrogen and found the (Cr,V,Nb) nitrides to be more soluble and less stable than carbides.

The *Z-phase* $(\text{Cr}_2\text{Nb}_2)\text{N}_2$ with a tetragonal structure generally is formed in type 347 steels with nitrogen contents above 0.06%, but has been detected as a minor phase at lower nitrogen levels. Like NbC, it requires high solution treatment temperatures and is stable when precipitated. Ayer *et al.* (33)

found it undissolved after 1h at 1027°C in an 18%Cr, 12%Ni steel with 0.3%Nb and 0.09%N. In steels with higher nitrogen contents it forms over a wide temperature range. Robinson and Jack (34) reported a solvus temperature above 1100°C for the Z-phase in the steel Rex 734, (0.05%C, 0.27%Nb, 0.38%N), Table 2. Vodarek (34) determined the morphology and orientation relationship for Z-phase formed in a modified 316L type composition (0.021%C with 0.30%Nb and 0.158%N). After solution treatment at 1300°C then reheating at 1100°C, the metallic content of the Z-phase particles was 61%Nb, 26%Cr, 8%Fe and 5%Mo. The relative stability of Nb(C,N) and Z-phase is discussed by Sourmail (21).

The h - M_6C carbide $(Fe,Cr,Mo)_6C$ or $(Fe_3Nb_3)C$ with a complex cubic structure is a non-strengthening, predominantly grain boundary precipitate which acts as a sink for chromium, molybdenum and niobium. As indicated by Minami *et al.* (36), it forms on ageing at temperatures between 600 and 800°C, Figure 1.

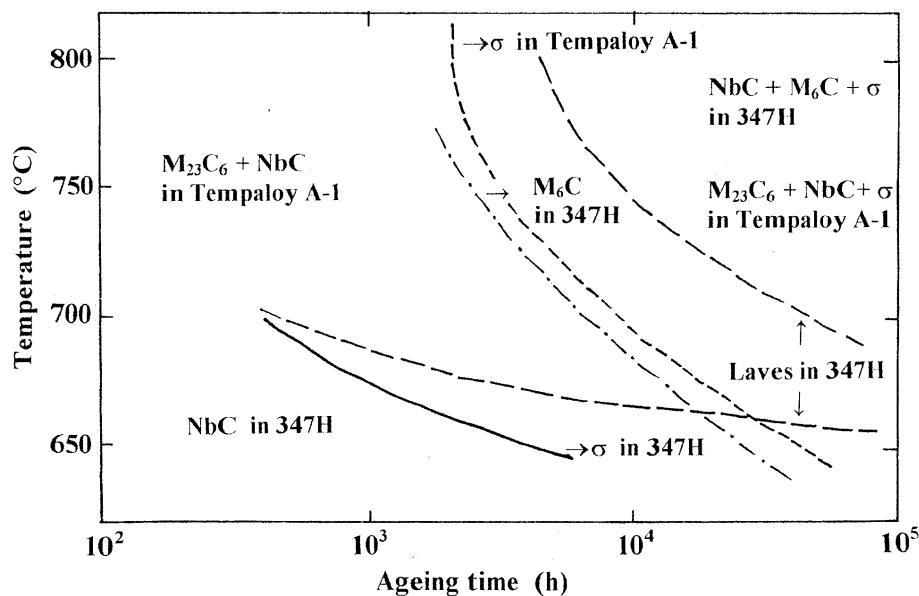


Figure 1: Phase transformations on ageing 347 and Tempaloy A-1 Nb,Ti steels, showing the range of Laves formation and the onset of M_6C in 347 and the delayed onset of sigma phase in the Nb,Ti steel compared with 347. (Ref. 36.)

Intermetallic and Other Precipitates

The *Laves* Fe_2Nb intermetallic phase with a hexagonal structure is again a phase inefficient in strengthening and acts as a sink for niobium. Both grain boundary and intragranular precipitation of Laves phase may take place at temperatures between 600 and 800°C in steels with high Nb:C ratios, Figure 1.

The b and g^* Ni_3Nb intermetallic phases are encountered in high niobium, high nickel austenitic alloys, Kirman (13) showed that they formed in solution treated and aged Fe-15%Cr alloys, replacing progressively the Laves phase at nickel contents above 25%. The g^* phase contributes significant precipitation hardening, but is metastable with respect to b . Since significant amounts of grain boundary Laves phase still form at 35% nickel, the g^* intermetallic strengthening process is more relevant to nickel-based alloys.

The *G-phase* silicide, with a complex cubic structure can be formed also with titanium. It has been reported as $Ni_{16}Nb_6Si_7$ in a 20%Cr, 25%Ni-Nb steel by Powell *et al.* (37), who gave C-curves for its precipitation on grain boundaries, with a nose at around 775°C. There is a possibility that some earlier identifications of M_6C in this alloy may have been of the G-phase, (21), (37). Ecob *et al.* (38) proposed a co-segregation process to explain the effect of increased oxygen and silicon contents in causing the instability of NbC relative to the G-phase. This instability leads to carbon rejection into the matrix.

The σ -Fe-Cr intermetallic may be an equilibrium phase over a range of service temperatures in compositions with high Cr equivalents. It usually forms on ageing first at grain boundary triple points and then on grain boundaries. It is generally regarded as detrimental, in terms of creep ductility, ambient temperature toughness and loss of matrix chromium. Niobium is considered to promote sigma phase formation, probably by acting as a ferrite stabiliser and reducing the loss of chromium from the matrix associated with $M_{23}C_6$ precipitation.

The $M_{23}C_6$ carbide, $(Cr,Fe,Mo,Ni)_{23}(C,B)_6$ has a complex cubic structure, is more soluble than the MX phases and normally is the first carbide to precipitate on grain and incoherent twin boundaries in unstabilised stainless steels. A stabilising addition of niobium, titanium or other strong carbide former is used to suppress $M_{23}C_6$ precipitation at grain boundaries. However, additions do not give immunity to formation of $M_{23}C_6$ on ageing after quenching from high solution treatment temperatures. Also, 'secondary' precipitation of $M_{23}C_6$ may occur as a result of release of carbon from transformation of NbC. Intragranular precipitation of $M_{23}C_6$ is beneficial for creep strength. The chromium carbides, although stabilised by molybdenum, coarsen more rapidly than either MX or Z-phase. Partial replacement of carbon by boron helps to stabilise both intragranular and grain boundary $M_{23}C_6$ precipitates and increases the density of grain boundary carbides, to the benefit of creep ductility, Harries and Shepherd (39). Boothby (15) found NbC and M_6C at the delta ferrite/gamma boundaries and intercellular ferrite/primary austenite boundaries in a 17%Cr, 11.5%Ni, 1.25%Mo weld metal, (0.015%C, 0.21%Nb, 0.01%Ti, 0.008%N). The presence of these carbides suppressed subsequent $M_{23}C_6$ carbide precipitation within the ferrite on ageing. The failure to reduce the matrix chromium content in the ferrite regions made them susceptible to intermetallic precipitate formation.

Niobium Carbide Solubility Considerations

The relative stabilities of NbC and NbN and solubility product relationships were discussed by Keown and Pickering (2) and by Sourmail (21), who cites the thermodynamically-based approach for determining solubility products advanced by Rios. Experimentally determined equations (2, 22) quoted for the 18%Cr, 10%Ni and 20%Cr, 25%Ni matrices are, respectively,

$$\log(Nb)(C) = -9350/T^* + 4.55 \quad (2)$$

$$\log(Nb)(C) = -8358/T + 4.07 \quad (3)$$

(*K)

These equations indicate a higher solubility in the 20%Cr, 25%Ni matrix. However, Kikuchi *et al.* (40) quoted an alternative relationship to equation 3,

$$\log(Nb)(C) = -7900/T + 3.42 \quad (4)$$

Minami and Kimura (41) give the relationship for combined additions of titanium and niobium to an 18%Cr-10%Ni matrix as:

$$\log (2\text{Ti}+\text{Nb})(\text{C}) = -7200/\text{T} + 3.3 \quad (5)$$

This indicates that a higher supersaturation can be developed with titanium present in the carbide. However, in estimating volume fractions, account must be taken of the variations in precipitate composition with time and temperature. Keown and Pickering (2) have discussed how the amount of niobium carbide available for precipitation at lower temperatures is reduced as the composition moves away from the stoichiometric ratio. As indicated by Powell *et al.* (37), below the nominal stoichiometric ratio of $\text{Nb}/(\text{C}+6/7\text{N}) = 7.7$ there is an increased tendency for the formation of M_{23}C_6 . Above 7.7 there is a tendency to form the M_6C carbide and, at ratios above 23:1, to form Laves phase. Kikuchi *et al.* (40) have observed that addition of niobium and titanium in excess of the solubility limits at the solution treatment temperature not only resulted in coarse particles but also resulted in faster coarsening of the secondary carbides.

Regrettably, there are few experimental determinations of solubilities for the more modern steels with multiple 'M' additions and for those with relatively high nitrogen to carbon ratios. As data for the relevant phases become available, thermodynamic approaches may help in the prediction of the relative stabilities and boundaries between the MC, M(CN) and Z phases.

Hot Working

The suppression of recovery and recrystallisation during hot working by niobium was recognised as a strengthening method in niobium austenitic steels for early gas turbine disc forgings. There have been numerous studies of the ductility troughs caused by dynamic precipitation of MC precipitates in tests involving high temperature solution treatment followed by reheating and straining. The comparatively early work of Barford and Myers (42) is discussed further below. Nakazawa *et al.* (43) used controlled rolling at relatively low temperatures, with niobium additions up to 0.2%, to strengthen compositions of the 304LN type. A 0.2% proof strength of over 650Mpa was achieved in 15mm plate, (0.06%C, 0.10%Nb, 0.18%N), rolling with 20-30% reduction in the temperature range 930-950°C. Lower rolling temperatures to develop warm worked structures have been advocated by, for example, Andreini *et al.* (44) for high strength manganese austenitic steels for non-magnetic drill collar (NMDC) applications.

Stabilisation

For stabilisation the matrix carbon content must be reduced to below a level at which a significant grain boundary area fraction of chromium carbides can form. Lower carbon levels allow use of reduced niobium additions, but the stabilisation ratio must increase as carbon falls. The chromium concentration gradient in the matrix near a grain boundary depends upon the temperature at which precipitation takes place and the extent of any back diffusion on subsequent ageing. 'Stabilisation ratios' are often set against experimental determination of corrosion susceptibility in a given medium. For example, Kajimura *et al.* (5) quote a minimum of 20:1 as the ratio for a 0.015%C, 25%Cr, 20%Ni steel for nitric acid service. Speidel (45) carried out stress corrosion crack growth rate tests

on low carbon and stabilised austenitic steels in a simulated 'faulted BWR' water at 288°C. Intergranular fracture was detected at the crack tips in the stabilised steels. However, better or similar crack growth rates were obtained for a sensitised '347LPN' steel with 0.013%C, 0.24%Nb, 0.063%N, when compared with a mill-annealed '316NG' with 0.017%C.

High temperature (~900°C) post welding stabilising treatments may be used to reduce the high local supersaturations of carbon and niobium resulting from weld cycles, see for example Kowaka *et al.* (46). Such treatments minimise the risk of intergranular stress corrosion cracking (IGSCC) for chemical plant components exposed to aggressive media on shut-down after operating at temperatures causing sensitisation. To obviate the use of PWHT, steels of the 347LN type, Table 1, can be used. These have a low carbon content, a high niobium stabilisation ratio and an enhanced nitrogen level for elevated temperature strength. Kudo *et al.* (47) have described the '347AP' variant of this type, with C<0.02% and an Nb/C ratio equal to or greater than 15. Nitrogen is added up to 0.1%, a limit set by the incidence of chromium nitrides. Ayer *et al.* (33) examined this alloy aged after high temperature solution and weld thermal cycle treatments. They concluded that the significant reduction in the incidence of the M₂₃C₆ carbide resulted from nitrogen retarding its precipitation.

Uno *et al.* (48) studied the sensitisation response of 0.04%C, 0.16%N, 18%Cr, 10%Ni steels containing relatively small amounts of niobium, titanium, zirconium or vanadium. With a 0.07% niobium addition, the Z-phase formed and could be taken into solution after 30 minutes at 1100°C. It formed as fine intragranular precipitates after solution treatment at 1000°C, with dislocation networks observed around the particles. Further precipitation occurred after ageing at temperatures between 650 and 900°C. At the higher ageing temperatures, M₂₃C₆ carbide was found to nucleate on the Z-phase. It was indicated that the inhibition of sensitisation noted in the niobium-nitrogen steel was related to trapping of carbon at the Z-phase-matrix interface. A similar precipitation sequence was noted at 800°C, in the modified alloy 800H examined by Diglio *et al.* (27).

Niobium-containing Creep Resistant Steels

Service Requirements

Nuclear reactor applications over a range of temperatures have determined much detailed alloy development. However, the conditions in the highest temperature/pressure locations in fossil fuel power generation steam circuits have also been a major factor. The strength advantages of the austenitic materials in conventional plant with metal temperatures below 575°C have been eroded by the development of improved ferritic and ferritic-martensitic stainless steels. Also, aggressive fireside corrosion conditions may limit use of homogeneous wrought steels. However, there is a continuing need for improved thermal efficiency, requiring materials for steam pressures and temperatures greater than in current 30MPa/600°C supercritical plant, Muramatsu (49), Kajigaya *et al.* (50). These conditions set targets for steels offering 10⁵h/100MPa rupture stresses at metal temperatures increasing from 650 to over 700°C. Differing oxidation conditions have led to families of steels based on, broadly, 13-18%Cr and 20-23%Cr.

In the creep deformation regime (at temperatures above ~500°C for austenitic steels in the absence of irradiation) the objectives are to develop a balance of creep strength with adequate creep rupture and room temperature ductilities. In addition, low cycle fatigue behaviour, creep strain and crack growth

rates, oxidation and hot corrosion resistance and initial and repair weldability must be considered. Relationships between stress, temperature, microstructure and deformation processes can be used to predict deformation and fracture paths and creep strain rates. As examples, Needham and Gladman (51) have provided deformation maps for a 347 and other 18%Cr 10%Ni steels. Harries (3) and Harries and Shepherd (39) have given summaries of creep processes.

The alloying principles for creep resistant steels for a given stress and temperature regime may be outlined. The matrix solid solution and the intragranular precipitate population provide resistance to dislocation creep. The presence of grain boundary precipitates and the nature of precipitates close to the boundaries determine grain boundary diffusion and sliding contributions to creep rate. Microstructural changes during service must not give rise to local regions of matrix weakness, harmful segregation or provide sites for cavitation and crack propagation at grain boundaries.

Intragranular Precipitation

Studies, for example by Keown and Pickering (2) and Evans *et al.* (52), attempted to quantify the relationships between intragranular MC precipitate population and creep resistance. This has been usually in terms of the transition from solute-drag to precipitate-dislocation interactions and the suppression of recovery, analysed in terms of the secondary creep rate and the stress exponent. These relationships are stress and temperature sensitive and of necessity many of these studies use short duration, high stress tests. The work of Fujiwara *et al.* (53) to relate soluble and precipitated niobium levels to creep strength indicated the effects from variations in grain size. Rupture strength for long service durations is often of primary practical interest and many studies have sought to optimise composition and microstructure against rupture strength.

The amount of precipitation of secondary 'NbC' in steels with relatively high ratios of C:N depends upon the supersaturation and approach to stoichiometry. Nucleation may take place on prior MX particles, grain boundaries, matrix dislocations, or at high supersaturations on stacking faults. Several workers have reported variability in the density of intragranular NbC precipitation in steels aged or creep tested from the solution anneal condition. Needham and Gladman (51) reported that, in both Type 347 and E1250 steels (Table 2) a boron addition caused the secondary NbC to be finer and more uniformly distributed after creep exposure at 650°C. They also found that pre-ageing the solution annealed Type 347 material for 1,500h at 650°C had little effect on the minimum creep rate and that the effect of creep strain on precipitation was dominant at that temperature in relatively high stress tests.

Generally, a moderate degree of cold work after solution annealing has been found to accelerate the initial MC precipitation and give a more uniform distribution, Swindeman and Maziasz, (54), Evangelista *et al.* (55). However, the magnitude of the effect is stress and temperature sensitive. For example, Piloni *et al.* (56) found that, in Type 347, 10% prestrain increased the creep strength at 750°C only in high stress tests. Controlled prior strain may be followed by an ageing, or stabilising, treatment significantly higher than the service temperature, as in the work of Powell *et al.* (37). For steels subject to irradiation, prior cold work is important, to improve both creep strength and resistance to void swelling.

Avoidance of recovery and the onset of primary recrystallisation, leading to the formation of regions of new, weak grains, sets a limit on the extent of prior cold work. This process has been described by

Harries (3). Evangelista *et al.* (55) observed a reduction in creep strength for Type 347 from the solution annealed condition after 15% cold work from this cause in tests at 825°C. Niobium-bearing steels are resistant to recovery through the pinning effects of NbC precipitation, up to about 750°C. Swindeman and Maziasz (31) reported the onset of recrystallisation at grain boundaries in a HT-UPS alloy 800H variant after creep at 700°C.

Barford and Myers (42) investigated the hot ductility of a Type 347 steel, in comparison with a 316 steel and the Mo,Nb,V,B steel E1250 (Table 2). In slow strain rate tensile tests, the intragranular MC precipitate was finer in the E1250 than in the Type 347 steel. The E1250 steel also showed recovery of the ductility loss induced by intragranular NbC precipitation on increasing temperature above 700°C, unlike the Type 347 steel. This recovery was attributed to a difference in the nature of the grain boundary precipitation. In the under-stoichiometric E1250 steel, the grain boundary and immediately adjacent regions were strengthened by $M_{23}C_6$ precipitation, unlike the weaker, precipitate-denuded regions seen in the Type 347 steel. Within the limitations of the examination methods available this work gives an early indication of the importance of the balance between intragranular and grain boundary precipitation.

The development of microstructures in thermally aged 347H and the lower Nb, Ti alloy were compared by Minami *et al.* (36) with those in 304H. The niobium-bearing steels were solution treated at 1100°C and aged for times up to 50,000h at temperatures in the range 650-800°C. The 304H steel showed predominantly grain boundary precipitation of $M_{23}C_6$ carbide, followed by grain boundary sigma phase formation. In the 347H steel both intragranular NbC and grain boundary sigma phase developed on ageing. The Laves phase was identified after sigma phase precipitation, followed by formation of an M_6C type carbide. At the higher temperatures the Laves phase was transient and the final structures developed at temperatures above 700°C consisted of the austenitic matrix, the two carbides MC and M_6C and sigma phase, Figure 1.

Källqvist and Andrén (23) found that NbC particle coarsening in their 347 steel was relatively slow at 700°C, reaching 40nm after 70000h. However, in a similar steel under creep deformation at the same temperature, this particle size was found after only 1,000h by Minami *et al.* (57). They compared precipitation on ageing a 347H and an 18%Cr-10%Ni 0.07% C, 0.13%Nb, 0.06%Ti steel with 0.033%N. The respective average MC particle sizes after 10,000h at 750°C in the two steels were around 80 and 45nm. They demonstrated that the significantly finer MC particle sizes with combined additions of titanium and niobium were maintained under creep conditions. The MC particles found in the Nb,Ti variant were consistently 50% smaller than those in the 347H after creep rupture testing over the range 100-80,000h at 700°C. In related work, Minami and Kimura (41) observed the co-precipitation of $M_{23}C_6$ and MC in an 18%Cr, 11%Ni, 0.12% C, 0.22%Nb, 0.01%N steel. They elucidated the relative contributions of the precipitates to creep strength at 650°C and found the MC precipitates to be more effective, reflecting their finer particle size, (10nm versus 100nm after 3,640h after creep to rupture at 700°C).

Maziasz and co-workers (30,31,54) have presented elevated temperature properties data for the (Nb,V,Ti)C,N strengthened HT-UPS steels with various matrix compositions. Kikuchi *et al.* (40) made a systematic study of the effects of carbon, niobium and niobium-titanium additions to the 20Cr-25Ni-0.05%N matrix. They used analysis of aged microstructures and creep rupture strengths at 700 and 750°C to identify an optimum strengthening precipitation regime. This optimum precipitation, of Nb(C,N) plus $M_{23}C_6$, was given by compositions which lay on the solubility curve for the austenitising temperatures used (1250°C) at an Nb/C ratio of 7.75 for the niobium addition and at the solubility

limits of the individual additions for the combined niobium and titanium additions (approximately 0.16%Nb and 0.11%Ti at 0.1%C). The beneficial effects on creep rupture strength from additions of molybdenum, nitrogen and boron were noted. This led to the formulation of the following composition range as a basis for maximum 10⁵h creep rupture strength:

0.05-0.15%C, 0.5%Si, 20%Cr, 25%Ni, 1.5%Mo, 0.2%Nb, 0.1%Ti, B, N.

Vodarek *et al.* (58) investigated niobium additions of 0.1 and 0.3%Nb to the 316LN steel (17Cr-12Ni-2.5Mo with 0.03%C, 0.15%N). After solution treatment at 1050 and 1120°C respectively the two alloys contained both grain boundary and intragranular Z-phase particles.

Z-phase precipitation continued during creep testing of these steels at 600 and 650°C, with mean particle sizes in the 0.3%Nb steel of 6 and 12nm after creep at 650°C for 81 and 37,890h respectively. Evans *et al.* (52) found a transition from MC to Z phases in a 20%Cr-25%Ni steel with 0.023%C, 0.41%Nb and 0.028%N. After solution treatment at 1150°C, the material was given 7% cold work and then aged at 850°C for 2 and 640h. After 2h only fine Nb(C,N) particles were observed, at 640h Z-phase formed, with a reduced volume fraction of finer NbCN particles.

Sawagari *et al.* (59) have described the development of the HR3C steel, Table 2, which has a 20%Cr, 25%Ni matrix strengthened with combined niobium and nitrogen additions to promote Z-phase precipitation. Araki *et al.* (60) reported the precipitation sequences observed in a 20%Cr, 25%Ni, 1.5%Mo steel containing 0.07%C, 0.26%Nb and 0.04%Ti with boron and an enhanced nitrogen level of 0.15%. This material was creep tested and aged at temperatures between 600 and 700°C. Intragranular precipitation of Z-phase was detected, with M₂₃C₆ and Cr₃Ni₂Si₂C forming both within the grains and on grain boundaries. The Z-phase precipitates remained significantly finer than the other phases. The Nippon Steel NF709 (61) is a related composition and examination of creep rupture specimens showed a similar precipitation population, Z-phase, M₂₃C₆ and Cr₃Ni₂Si₂C with traces of Nb(C,N) being reported only transiently at temperatures below 700°C and present for times out to 10⁴h at 600°C. Figure 2 allows comparison of the stability of the precipitate particles formed in creep-ruptured specimens after exposure at 700°C.

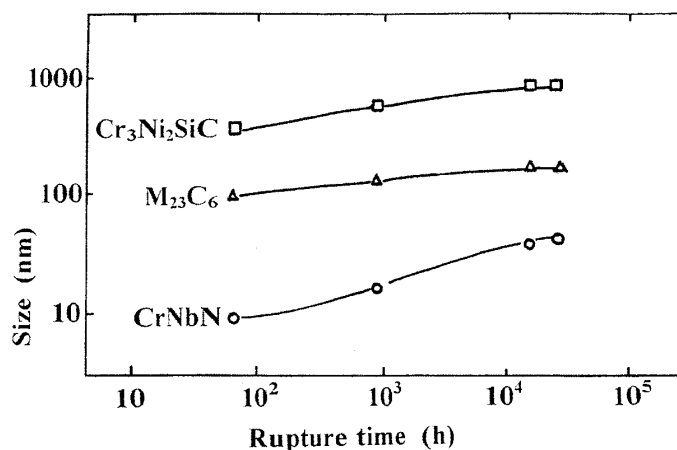


Figure 2: Comparison of precipitate particle sizes developed in creep of the NF709 steel, over a range of rupture times at 700°C, (Nippon Steel Co. Technical Information) (61).

To achieve the higher creep rupture strengths, carbide and nitride intragranular precipitation can be supplemented by the use of copper. Kimura and Minami (62) give a time-temperature-precipitation diagram for a 17%Cr, 14%Ni, 3%Cu, 2.5%Mo steel containing 0.11%C, 0.4%Nb, 0.2%Ti and a boron addition. The 3% copper addition was found to give precipitation of a Cu-rich phase over the temperature range 600-800°C, increasing the creep rupture strength given by the MC and $M_{23}C_6$ precipitates. The precipitation sequence at 750°C was $M_{23}C_6$, 'Cu', MC and Fe_2Mo . The 18%Cr, 10%Ni, 3%Cu steel with 0.10%C, 0.3%Nb, 0.15%Ti steel and a boron addition, reported by Tohyama *et al* (63) gave a similar precipitation sequence without the Laves phase. A further copper-containing variant, the 'Super 304H' described by Sawagari *et al.* (64) is based on a 0.10%C, 18%Cr, 9%Ni, 3%Cu, 0.4%Nb, 0.1%N composition. The precipitates reported for this steel were, Nb(C,N), $(Cr,Nb)_2N_2$, $M_{23}C_6$ and, at 700°C, 'Cu'.

Grain Boundary and Intermetallic Precipitation

The microstructures in thermally aged 347H and the Nb-Ti alloy Tempaloy A-1 (Table 2) were compared by Minami *et al.* (36) with those in 304H. The niobium-bearing steels were solution treated at 1100°C and aged for times up to 50,000h at temperatures in the range 650-800°C. The 304H steel showed predominantly grain boundary precipitation of $M_{23}C_6$ carbide, followed by grain boundary sigma phase formation. In the 347H steel grain boundary sigma phase developed on ageing, Figure 1. The Laves phase was identified after sigma phase formation, followed by formation of an M_6C type carbide. At the higher temperatures the Laves phase was transient and the final structures developed at temperatures above 700°C consisted of the austenitic matrix, sigma phase and the two carbide variants MC and M_6C . The niobium-titanium steel showed later precipitation of a lower level of sigma phase formation than in the 347H material. Both steels in this study were relatively fine-grained. The lower sigma phase levels in the niobium-titanium steel were attributed less to grain boundary area effects than to the differences in composition, and hence in phase stability.

In a 0.3%Nb 316LN steel Vodarek *et al.* (58) found that the Laves phase formed rapidly and $M_{23}C_6$ carbide was replaced subsequently by $M_6(C,N)$ and then sigma. Similar phase sequences were noted both at the grain boundaries and within the grains, but there were greater amounts of $(M)_6(C,N)$ and sigma at the grain boundaries.

Powell *et al.* (37), determined the ageing characteristics of a 20%Cr, 25Ni% steel containing 0.037%C, 0.68%Nb (with 0.055%Ti, 0.01%N, 0.61%Si) and given a 'Recovery Anneal' treatment. This involved a 1050°C anneal, followed by 30% cold work, a 930°C/1hr anneal, then 3% cold strain and a further 930°C/1hr anneal. The microstructure produced contained matrix and grain boundary Nb(C,N) with a residual dislocation distribution. Ageing at 650°C brought about a transformation of grain boundary Nb(C,N) to G-phase, the resultant rejection of carbon leading to the formation of $M_{23}C_6$, followed by sigma, possibly accelerated by the local loss of nickel from the matrix. Within the grains further fine Nb(C,N) precipitates formed, followed by G and sigma phases but at longer times. The same sequence was observed in material annealed at 930°C/1hr without the 3% cold work, but the transitions were delayed and no matrix sigma phase was detected after 10,000h.

Control of Austenite Grain Size

In addition to providing sites for precipitation and recrystallisation, the grain structure influences other aspects of behaviour. Large grain sizes are of advantage in reducing the creep strain contribution from grain boundary diffusional processes. They also reduce the grain boundary area for precipitation. However, they are detrimental to rupture ductility and room temperature toughness. Also, in high

temperature steam circuits, steam-side oxidation is a major factor, as it controls the heat flux through tube walls. A fine grain size aids the rapid build-up of a chromium-rich protective film and reduces oxide exfoliation. High rupture strength requires maximising the amount of uniformly distributed, stable, fine intragranular precipitation. However, for many MX precipitating systems the use of a high final solution treatment temperature leads to secondary recrystallisation and a coarse grain size. An effective compromise is to use a controlled, two-stage solution treatment incorporated into the manufacturing route for the tube or plate product. This has been found particularly effective for the Type 347 steel. Teranishi *et al.* (65) have described such a treatment; a high penultimate solution anneal, followed by controlled cold working and then a normal solution anneal. They demonstrated that this 'HFG' treatment gave little difference in the final strengthening NbC volume fraction compared with normal treatments, despite achieving a change in grain size from around ASTM4-5 to 8. Creep rupture strengths were superior to those of conventionally treated steels and there was a significant improvement in creep-fatigue.

The improvements sought in the efficiency of gas turbine-based energy cycles, particularly for small units, has led to intensive work on suitable exhaust gas-input air heat exchange systems operating at around 650°C. The ductility, elevated temperature strength and oxidation resistance of the Type 347 steel are of benefit in the manufacture of the thin-walled (0.1mm) primary surface recuperators. Foil annealing using the principles of the HFG treatment has been proposed by Maziasz *et al.* (66), to develop a fine grain size and optimum creep strength. However, although fine grain sizes aid the rapid development of a protective layer, continuous transport of chromium to the surface of a thin foils can result in significant chromium matrix depletion.

Summary of the Development of the Creep-resisting Steels

The sequence of alloy development for the niobium steels for power generation service is illustrated in plots of allowable design stress versus temperature in Figure 3.

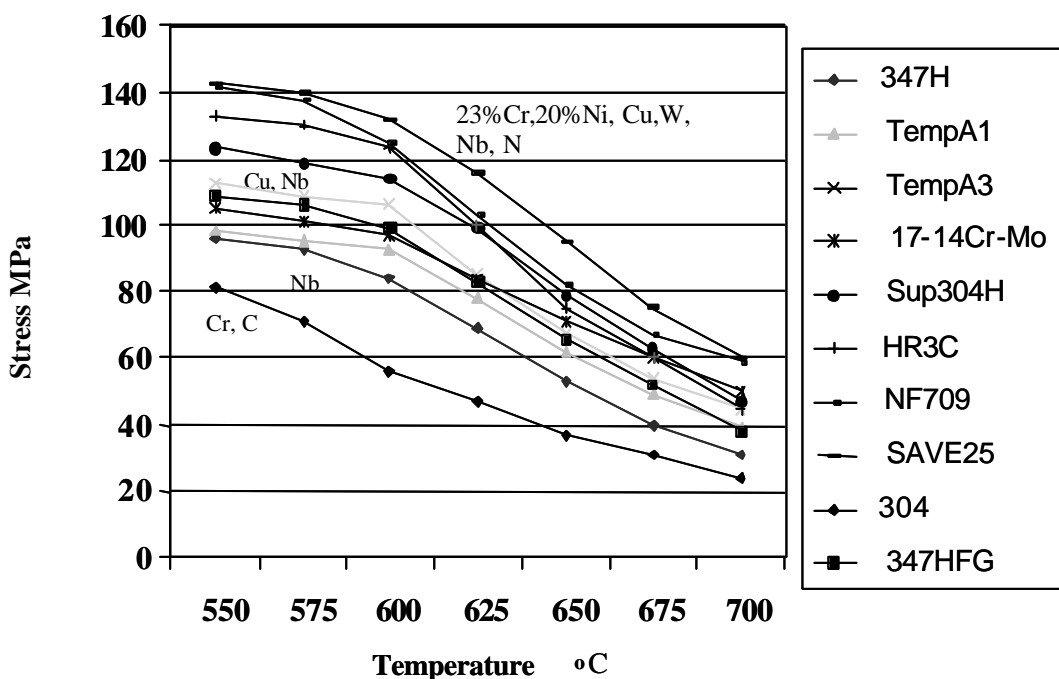


Figure 3. Allowable Design Stress values for selected niobium-bearing steels as a function of temperature, (29, 49, 59, 60, 61, 63).

The metallurgical principles, based on the microstructural studies outlined above, can be summarised in relation to the steels as follows. The 347H with a specified minimum carbon content represented the first step towards controlled high temperature properties. The double heat treatment of the 347HFG counters the problem of the high solution treatment temperatures required to develop NbC precipitation and confers advantages in both steam-side oxidation and rupture strength. The advantages of the combined niobium-titanium addition for strength may be seen, with the benefits of a reduction in the amount of insoluble NbC and the propensity to form sigma phase. Reduced niobium and carbon levels combined with enhanced nitrogen contents give mixed carbide-nitride precipitation sequences, to which can be added copper.

For the intragranular precipitates, particle size, number and stability appear to be more important than particle chemistry, as evident from the use of mixed MC, $M_{23}C_6$, Z-phase and 'Cu' precipitation. For the niobium-interstitial phases, the order of stability in terms of growth rates appears to be Z-phase > 'alloyed MC' > NbC > $M_{23}(CB)_6$. However, account needs to be taken of the sequence of precipitation, particularly where $M_{23}(CB)_6$ can form as the result of 'secondary' sources of carbon. Uniformity of distribution of these particles is essential, to avoid strain concentrations, particularly adjacent to grain boundaries. Grain boundary particles must be effective in preventing grain boundary sliding and diffusion and not destabilise the structure by decomposition. A comparison on design stress alone is simplistic. Many other issues, including constraints set by heat treatment and fabrication, affect comparisons between steels. For example, some steels require relatively high solution treatment temperatures. However, the family of niobium-containing steels reviewed has been developed with these constraints in mind.

Niobium in Cast Austenitic Stainless Steels

In addition to the cast equivalents of the standard niobium stabilised austenitic grades and those designed for corrosion resistance, there is an important family of heat resisting cast steels used in the petrochemicals industries. These operate at temperatures of 850-1050°C in steam reformer tubes and at temperatures of 1100°C in pyrolysis heater tubes. One such alloy with good ductility and adequate weldability is the 1.4859 low carbon 20%Cr, 32%Ni, 1.2%Nb steel, Table 1. Cox, cited by Wen-Tai and Honeycombe (67) showed how the creep rupture properties and scaling resistance of this grade could be improved by reducing the niobium content and very similar properties could be achieved with a 19%Cr, 26%Ni, 0.55%Nb steel.

Higher carbon steels have been established for related applications where ductility is less important, for example the HK40 25%Cr-20%Ni-1%Si composition. In centrifugal and other castings at relatively high solidification rates, the primary carbide M_7C_3 is formed, in eutectic networks. Subsequent transformation of this carbide to $M_{23}C_6$ liberates carbon which can form secondary $M_{23}C_6$ precipitates, particularly in matrix regions adjacent to the eutectic networks.

Shinoda *et al.* (68) investigated the effects of single and combined additions of titanium and niobium to the HK40 steel. They sought to optimise both the morphology and volume fraction of the eutectic networks and the extent and stability of the secondary carbide precipitation. The eutectic network morphology was found to influence the tertiary creep stage through rates of cavity nucleation and crack propagation. The interactions of modification to the primary carbides and secondary precipitation in the matrix led to definition of Ti or Nb/C atomic ratios of 0.5 up to around 1 for a considerable improvement in creep rupture strength by a single alloying addition. Further improvements were obtained with a combined addition and this work identified two compositional

criteria, in the form of atomic % ratios, for optimisation of creep rupture strength by the combination of Nb and Ti. The first of these determines the secondary carbide precipitation and the second the network morphology. The composition of their optimum steel is given in Table 1.

$$(Ti+Nb)/C \text{ and } Ti/(Ti+Nb) \text{ both} = 0.3$$

Tai and Honeycombe (67) also investigated the microstructural effects of the additions of stabilising elements to this composition. Combined (Nb,Zr) and (Nb,Ti,Zr) additions were used in an attempt to confer additional creep rupture strength. The (Nb,Ti,Zr) addition was the most effective, because of modification of the eutectic niobium carbides from a lamellar to a granular morphology and the greater resistance of the secondary (NbTiZr)C precipitates to coarsening during creep. Stacking-fault precipitation of MC was observed, a consequence of the high supersaturation given by the presence of titanium. The stability of this mode of precipitation contributed to the improvement in rupture strength.

Ibanez *et al.* (69) studied 0.4% C 20% Cr-33% Ni-2% Nb alloys, finding that the as-centrifugally cast structure consisted of eutectic NbC and massive particles of Cr₇C₃, with M₂₃C₆ present in a similar composition when statically cast. In these alloys, ageing at temperatures between 850 and 980°C results in the replacement of the Cr₇C₃ carbide by M₂₃C₆, secondary precipitation of M₂₃C₆ and NbC, with replacement of some of the pre-existing NbC by the Ni₄₆Nb₆Si₇ G-phase. The initial volume fraction of NbC and its rate of transformation to G-phase were found to increase with the silicon content. The transfer of the niobium into the G-phase can result in the further formation of secondary chromium carbides. NbC transformation was accelerated by increasing the silicon content and the time to rupture was improved by presence of the G-phase. However, high silicon contents incurred the risks of ferrite and sigma phase formation.

Oxidation

Baxter and Natesan (70) found beneficial effects from relatively high niobium additions (up to 6%) to 12 and 25% Cr austenitic alloys. The additions aid the early formation of chromium-rich layers. A discrete layer of Nb₂O₅ could be formed at the metal-oxide interface under Cr₂O₃ in oxidising conditions and a mixed (Nb,Cr) oxide may develop. At low oxygen partial pressures higher niobium contents were required for the protective effect. For the 25% Cr-20% Ni Type 310 steel the presence of niobium induced a relative increase in the initial rate of oxidation, allowing protective oxide layers to develop. Incorporation of niobium into a pre-formed oxide scale on the 3 and 6% niobium steels was found to delay the onset of scale breakdown on subsequent exposure to sulphur-bearing gases in simulated coal gasifier atmospheres. Niobium was detected at the metal/metal oxide interfaces with increasing niobium content.

Ramanathan *et al.* (12) studied the effect of niobium (0.44, 0.89 and 1.88%) on the oxidation of 15% Cr, 15% Ni austenitic steels. Tests at 800 and 900°C showed that the overall extent of oxidation was reduced with increasing niobium content. The scaling index derived from the cyclic tests at 900 and 1100°C increased with increasing temperature and decreased with increasing niobium content. Niobium was detected at the metal/metal oxide interfaces with increasing niobium content and the effect was attributed to niobium in solid solution facilitating the formation of Cr₂O₃.

Alloys Subject to Irradiation.

Niobium-bearing austenitic stainless steels have been used widely in components for nuclear systems. A major concern for within-core components has been to minimise degradation in the form of embrittlement, loss of creep strength and physical distortion of components (particularly in austenitic alloys) resulting from void formation and swelling. Segregation patterns, precipitation sequences and kinetics are modified by radiation-induced point defects. Impurity atoms may be generated from transmutations, for example the internal generation of helium. Radiation damage effects and measures to optimise microstructures have been reviewed by Harries and Shepherd (39).

Point defect movement can lead to migration of chromium away from and nickel towards grain boundaries, one form of radiation induced segregation (RIS). This may result in destabilisation of the austenite matrix by depletion in nickel through grain boundary precipitation and increased susceptibility to stress corrosion cracking as a result of localised chromium depletion. Oversize matrix solute atoms such as niobium can bind with vacancies and slow the migration process. Kato *et al.* (18) have advanced a ranking of the effect of the elements Hf, Zr, Ta, Nb, Ti and V in solution, on the basis of atomic size difference, and identified an optimum addition of 0.5-0.9% Nb in Types 304 and 316-based compositions.

Formation of a fine dispersion of stable MC particles provides means of trapping both voids and helium bubbles within the grains and a suitable particle dispersion at the grain boundaries can reduce cavitation and void formation. Titanium additions have been widely used, but particle stability can be optimised with multiple alloy additions.

For exposure to the high fluences anticipated in conceptual fusion reactor designs, the relative void swelling characteristics of austenitic steels are considered a disadvantage. Activation of the reactor structure will govern plant radioactive waste storage and disposal strategies and costs. Isotopes and the resulting activation produced by individual elements on irradiation can be predicted (in the case of niobium, ^{94}Nb). Assumptions as to acceptable activation/handling and storage time/disposal options allow elements to be ranked. Certain 'Low Activation' alloy development programmes for both austenitic and ferritic or martensitic stainless steels require the elimination of niobium.

In Conclusion

Although most recently-developed steels make use of multiple 'microalloying' additions, niobium retains an important role amongst alloying elements making the austenitic stainless steels a versatile family of materials. Niobium-bearing grades have maintained their positions in a range of applications and there have been progressive improvements in their performance. These have been achieved mainly by applying well-established metallurgical principles, together with the information available from modern metallographic and analytical methods. The optimisation methods used in recent years have remained founded on experimental observation, testing and validation. However, a future review may well devote far more attention to the results of modelling methods applied to alloy design. Maziasz (30) has summarised some of the principles established for compositional design and thermodynamic models for structure prediction, based on phase stability, interfacial energies and matrix diffusion mechanisms, are under intensive development.

Acknowledgements

The author's sincere thanks to the Institute of Materials and Nippon Steel for use of figures and to the many people who have taken time to respond to enquiries, in particular to my friends in AvestaPolarit and J. Källqvist, KTH for her private communication.

References

- (1) W. O. Binder in R. A. Grange *et al.* Boron, Calcium, Columbium and Zirconium in Iron and Steel (NewYork/London: Wiley 1957), 210-395.
- (2) F. B. Pickering and S. R. Keown, Niobium, Proceedings of the International Symposium ed. H. Stuart, (Warrendale, PA: Met. Soc. AIME (1981), 1113-1142.
- (3) D. R. Harries, "Physical metallurgy of Fe-Cr-Ni Steels," Mechanical Behaviour and Nuclear Applications of Stainless Steels at Elevated Temperatures, Varese 1981 (The Metals Society, London, 1982), 1-21.
- (4) D. J. Kotecki and T. A. Siewert, "WRC-1992 constitution diagram for stainless steel weld metals: A modification of the WRC-1988 diagram," Welding Journal (Research Supplement), 71 (5) (1992), 171-178
- (5) H. Kajimura, K. Ogawa and H. Nagano, "Development and modification of stainless steels for nuclear fuel reprocessing plants," Stainless Steels '94, (Gothenburg, Sweden, Chalmers 1994), 786-794.
- (6) J-O. Nilsson, "The physical metallurgy of duplex stainless steels," Proc. 5th World Conference, Duplex Stainless Steels '97 (Zutphen, Holland: KCI 1997), 73-82.
- (7) S. M. Rossitti and J. M. D. A. Rollo, "Phase precipitation in a niobium-containing cast duplex stainless steel," Metalurgia and Materials ABM 54 (1998), 293-302.
- (8) G. Tacke and H. J. Kohler, "Precipitation behaviour of ferritic-austenitic stainless steels of high molybdenum content," Steel Research 58 (1987), 123-128.
- (9) W. Stasko and E. J. Dulis, "New automotive valve steels with improved properties," High Manganese High Nitrogen Austenitic Steels (Ohio, USA, ASM 1987), 43-52.
- (10) E. Folkhard, Welding Metallurgy of Stainless Steels, (Vienna/NY Springer, 1984).
- (11) A. W. Denham and J. M. Silcock "Precipitation of Fe₂Nb in 16%Ni-16%Cr steel and the effect of Mn and Si additions," JISI, 207 (5) (1969), 585-592
- (12) L. V. Ramanathan, M.Pohl, and A. F. Padilha, "The effect of niobium addition on the microstructure of fully austenitic Fe-15Cr-15Ni stainless steels," Materials and Corrosion, 46 (1995), 71-75.

- (13) I. Kirman, "Precipitation in the Fe-Ni-Cr-Nb system," ibid. ref 11, 1612-1618.
- (14) A Guide to the Solidification of Steels (Stockholm, Sweden Jernkontoret, 1977), 98-101.
- (15) R. M. Boothby, "Solidification and transformation behaviour of Nb-stabilised austenitic stainless steel weld metal," Mats.Sc.&Tech. 2 (1) (1986), 78-87.
- (16) C. D. Lundin, "Fabrication and service related weldability of austenitic stainless steels," Conf on Stainless Steels '91, Chiba. (Tokio, Japan, ISIJ, 1991), 961-973.
- (17) B. S. Lee *et al.*, "J-R fracture properties of SA508-1a ferritic steels and SA312-TP347 austenitic steels for pressurised water reactor's (PWR) primary coolant piping," Nuclear Engineering. & Design, 199 (2000), 113-123.
- (18) T. Kato *et al.* European Patent Application 0 530 735 A1, (1992).
- (19) L. G. Martinez, *et al.*, "Influence of niobium on stacking-fault energy of all-austenite stainless steels," Steel Research 63 (5) (1992), 221-223.
- (20) A. W. Marshall and J.C.M. Farrar, "Effects of residual, impurity and microalloying elements on properties of austenitic stainless steel weld metals," Metals Construction 16 (6) (1984), 347-353.
- (21) T. Sourmail, "Precipitation in creep resistant austenitic stainless steels," Mats.Sc.&Tech. 17 (1) (2001), 1-13.
- (22) M. Deighton, "Solubility of NbC in 20%Cr-25%Ni stainless steel," JISI 205 (5) (1967), 535-538.
- (23) J. Källqvist and H-O. Andrén, "Development of precipitate size and volume fraction of niobium carbonitrides in stabilised stainless steel," Mats. Sc. & Tech. 16 (10) (2000), 1181-1185.
- (24) J. Källqvist and H-O. Andrén, "Microanalysis of a stabilised austenitic stainless steel after long term ageing," Mats. Sc. & Eng. A270 (1999), 27-32.
- (25) J. Källqvist, Chalmers University of Technology, Gothenberg, Sweden, private communication, May 2001.
- (26) H-O Andren, A. Henjered and L. Karlsson, "MX precipitation in stabilised austenitic stainless steels," Stainless Steels '84, (London, England IoM 1985), 91-96.
- (27) M. R. Diglio *et al.*, "Creep behaviour and metallurgy of modified 800H," in High Temperature Materials for Power Engineering (Dordrecht, Holland, Kluwer 1990), 545-554.
- (28) M. Schwind *et al.*, "Nitrogen uptake during creep testing of an austenitic stainless steel," Proceedings EUROMAT 2001 Rimini, (June 2001)

- (29) A. Tohyama and Y. Minami, "Development of the high temperature materials for ultra super critical boilers (NKK Tempaloy series)," Advanced Heat Resistant Steels for Power Generation (London, England IoM, 1999), 494-506.
- (30) P. J. Maziasz, "Developing an austenitic stainless steel for improved performance in advanced fossil power facilities," JOM 41 (7) (1989), 14-20.
- (31) R. W. Swindeman and P. J. Maziasz, "The effect of MC forming additions and 10% cold work on the high temperature strength of 20Cr-30Ni-Fe Alloys," K. Natesan and D. J. Tillack, Heat Resistant Materials, Proceedings of the 1st Int. Conference (Ohio, ASM_Int. 1991), 251-259.
- (32) T. Thorvaldsson and G. L. Dunlop, "Effect of stabilising additions on precipitation reactions in austenitic stainless steels," Met.Sci. 16 (4)4 (1982), 184-190.
- (33) R. Ayer, C. F. Klein and C. N. Marzinsky, "Instabilities in stabilised austenitic steels," Met. Trans. A 23 (9) (1992), 2455-2467.
- (34) P. W. Robinson and D. H. Jack, "Precipitation of Z-phase in a high-nitrogen stainless steel," in New Developments in Stainless Steel Technology ed. R. Lula (Ohio, ASM 1985), 71-76.A.
- (35) V. Vodarek, "Morphology and orientation relationship of Z-phase in austenite," Metall. Mater., 29 (4) (1991), 229-235.
- (36) Y. Minami, H. Kimura and Y. Ihara, "Microstructural changes in austenitic stainless steels during long term ageing," Matls. Sc.&Tech. 2 (8) (1986), 795-806.
- (37) D. J. Powell, R. Pilkington and D. A. Miller, "The Precipitation characteristics of 20-25Nb stabilised stainless steel," Acta Met. 36 (3) (1988), 713-724.
- (38) R. C. Ecob, R. C. Lobb and V. L. Kohler, "The formation of G-phase in 20/25 Niobium stainless steel AGR fuel cladding alloy and its effect of creep properties," J. Mater.Sci. 22 (1987), 2867-2880.
- (39) D. R. Harries and C. M. Shepherd, "Creep-rupture ductilities of austenitic steels," Rupture Ductility of Creep Resisting Steels ed. A. Strang, (London, Institute of Metals, 1991), 246-267
- (40) M. Kikuchi *et al.*, "An austenitic heat resisting steel tube developed for advanced fossil steam plants," Proceeding of an International Conference on Creep (Tokyo, JSME 1986), 215-220.
- (41) Y. Minami and H. Kimura, "Effect of and MC Carbides on creep rupture strength of 10%Cr-10%Ni-Ti-Nb Steel," Trans.ISIJ 27 (4) (1987), 299-301.
- (42) J. Barford and J. Myers, "Structure related to hot ductility of three austenitic steels," JISI 201 (12) (1963), 1025-1031.
- (43) T. Nakazawa *et al.* "Development of high strength stainless steels for high speed ships," Nippon Steel Tech. Rep. 71 (1996), 45-52.

- (44) R. J. Adreini, A. J. Farmer and S. Yabuchi, US Patent 4523951, (1985).
- (45) M. O. Speidel, "Stress corrosion cracking of titanium- and niobium stabilised austenitic stainless steels in 288°C water," Paper No.132 (Houston, NACE 1994).
- (46) M. Kowaka, T. Kudo and K. Ota, "Intergranular stress corrosion cracking of 18-8Ti and 18-8Nb stainless steels in polythionic acid solution," Environment-sensitive fracture of Engineering Materials (Chicago, 1977), 178-190.
- (47) T. Kudo *et al.*, "347AP Stainless Steel with high resistance to polythionic Acid SCC for Furnace Tubes," Sumitomo Search, 36 (5) (1988), 73-82.
- (48) H. Uno, A. Kimura & T. Misawa, "Effect of Nb on the Intergranular Precipitation Behaviour of Cr Carbides in N-bearing Austenitic Stainless Steels," Sumitomo Search, 54(10) (1993), 48-55.
- (49) K. Muramatsu, "Development of ultra-super critical plant in Japan," *ibid.* ref.29, 543-557.
- (50) I. Kajigaya *et al.*, "Service Experience with the application of advanced materials in improved coal fired power plants operating in the range 593-610°C. *ibid.* ref. 29, 172-183.
- (51) N. G. Needham and T. Gladman, "Creep Mechanisms". Final Report on ECSC Project 6210.MA/8/801, (British Steel Corporation Sheffield Laboratories, England, 1977.)
- (52) H. E. Evans, G. Knowles and G. L. Reynolds, "Convergence of creep strengths at high strain rates in particle-strengthened steels," Creep and Fracture of Engineering Materials and Structures, Vol.1. (Pineridge, Swansea UK 1984), 245-254.
- (53) M. Fujiwara, H. Uchida and S. Ohta, "Effect of niobium content on creep strength of cold-worked 15Cr-15Ni-2.5Mo austenitic steel," J.Matls.Sc Let. 14 (1995), 297-301.
- (54) R. W. Swinderman and P. J. Maziasz, "The mechanical and microstructural stability of austenitic stainless steels strengthened by MC-forming elements," 5th Int. Conf. On Creep of Materials (Ohio, USA ASM 1992), 33-42.
- (55) E. Evangelista *et al.*, "Cold work effect on particle strengthening in creep of an AISI 347 stainless steel," Materials for Advanced Power Engineering, ed. D. Courtsouradis *et al.* (Holland, Kluwer Academic 1994), 485-493.
- (56) G. Pilloni, E. Quadri and S. Spigarelli, "Interpretation of the role of forest dislocations and precipitates in high temperature creep in a Nb-stabilised austenitic stainless steel," Matls.Sci.&Eng. A279 (2000), 52-60.
- (57) Y. Minami, H. Kimura and M. Tanimura, "Creep rupture properties of 18%Cr-8%Ni-Ti-Nb and Type 347H austenitic stainless steels." New Developments in Stainless Steel Technology, Detroit, Michigan, USA, 13-21 September, 1984,231-242.

- (58) V. Vodárek *et al.*, "Effect of niobium on the microstructure and creep properties of AISI 316LN type steels," Applications of Stainless Steels '92 eds. H. Nordberg, J. Björklund, (Stockholm, Sweden, Jernkontoret 1999), 123-132.
- (59) Y. Sawagari *et al.*, "The development of HR 3 C steel with high elevated temperature strength and high corrosion resistance for boiler tubes," Sumitomo Metals 37 (2) (1985), 66-78.
- (60) S. Araki *et al.*, "Behaviours of microstructures and precipitates during creep and ageing of high strength 20Cr-25Ni steel for tubes in Ultra-Supercritical Power Boilers." Microstructures and Mechanical Properties of Aging Material eds. P. K. Liaw *et al.* (TMMS 1993), 99-105.
- (61) "Quality and Properties of NF709 austenitic stainless steel for boiler tube applications," (Brochure, Nippon Steel Corp. Tokyo, Japan 1996)
- (62) H. Kimura and Y. Minami, "Precipitation of Cu-rich phase in 17-14CuMo stainless steel during creep and high temperature aging," Trans ISIJ, 25 (11) (1985), B312.
- (63) A. Tohyama, M. Miyauchi and Y. Minami, "Development of 18Cr-10Ni-3Cu-Ti-Nb stainless steel for ultra super critical boilers," *ibid.* ref. 60, 495-504.
- (64) Y. Sawagari *et al.*, "Development of the economical 18-8 stainless steel (Super 304H) having high elevated temperature strength for fossil fired boilers," Sumitomo Search 48 (1) (1992), 50-58.
- (65) H. Teranishi *et al.*, "Fine-grained TP347H steel tubing with high elevated temperature strength and corrosion resistance for boiler applications," Sumitomo Search, 38 (5) 1989, 63-64.
- (66) P. J. Maziasz *et al.*, "Stainless steel foil with improved creep resistance for use in primary surface recuperators for gas turbine engines," Conf. Proc. Gas Turbine Materials Technology (Ohio, ASM Int. 1999), 70-78.
- (67) Hou Wen-Tai and R. W. K. Honeycombe, "Structure of centrifugally cast austenitic Stainless Steels: Parts 1&2, Effects of Nb, Ti and Zr," Matls. Sc. & Tech. 1, (1985), 385-389, 390-397.
- (68) T. Shinoda *et al.*, "The Effect of Single and Combined Additions of Ti and Nb on the Structure and Strength of the Centrifugally Cast HK-40 Steel," Trans. ISIJ 18 (1978), 139-148.
- (69) R. A. P. Ibanez *et al.*, "Effects of Si content on the microstructure of modified-HP austenitic steels," Matls. Characterisation 30 (1993), 243-249.
- (70) D. J. Baxter and K. Natesan, "The oxidation-sulphidation behaviour of Fe-Cr-Ni-Nb alloys at elevated Temperatures," Corrosion, Erosion, Wear of Materials at Elevated Temperatures (Houston, USA, NACE, 1986), 309-323.